Arch. Metall. Mater. **64** (2019), 4, 1661-1666

DOI: 10.24425/amm.2019.130141

C. SUCHOCKI*#, D. MYSZKA**, K. WASILUK***

# TRANSFORMATION KINETICS OF AUSTEMPERED DDUCTILE IRON: DILATOMETRIC EXPERIMENTS AND MODEL PARAMETER EVALUATION

In this study a group of selected transformation kinetics equations is applied to describe the isothermal ferritic transformation in austempered ductile iron (ADI). A series of dilatometric tests has been carried out on ADI at different temperatures. The obtained experimental data are utilized to determine the parameter values of the considered kinetic equations. It is found that the transformation kinetics models by Starink, Austin and Rickett are substantially more effective at describing the ferritic transformation in ADI than the much celebrated Johnson-Mehl-Avrami-Kolmogorov (JMAK) equation. Furthermore, it is demonstrated that evaluating the kinetic parameters using the least squares method instead of calculating them from vastly used formulas can significantly improve the accuracy of the JMAK model's predictions.

*Keywords:* ADI, transformation kinetics, diffusional transformation, model characteristics

## 1. Introduction

A proper mathematical description of the phase growth plays an important role in modeling quenching and hot forming processes [1,8]. It has influence not only on the theoretical predictions of material microstructure evolution during a selected technological process, but also on the simulated residual stresses and strains. Thus, a correct choice of transformation kinetics equation and determination of its parameters become an important problem [1,2].

In this study, a number of dilatometric experiments is reported that have been conducted in order to assess the ferrite growth in ductile iron for selected temperatures of austempering. A chosen group of kinetic equations has been applied to describe the isothermal ferrite growth which takes place during the austempering process. The conclusions which are drawn from the presented results can contribute to a more effective modeling of the transformation kinetics in ductile iron.

## 2. Materials and methods

### 2.1. Transformation kinetics in austemepered ductile iron

The studies on transformations and their impact on the structure and properties of austempered ductile iron boil down to the analysis of phenomena during the heat treatment cycle, consisting of austenitizing and austempering. Austenitizing primarily determines the carbon content in austenite, while the isothermal transformation which follows the rapid cooling from the austenitizing temperature ultimately shapes the ADI's structure.

The temperature and time of austenitization determine the carbon content in the ductile iron matrix. By setting the temperature at a given level, the value of the equilibrium carbon concentration in austenite can be adjusted, whereas the time decides if and when this moment will occur. The higher the austenitizing temperature, the faster the carbonation of austenite occurs. The solubility of carbon from graphite nodules also increases with temperature. Austenite becomes more homogeneous and its grains grow more [4,9,14]. However, the final shaping of the structure occurs during the next step of heat treatment – the austempering. At this step the isothermal transformation in ductile iron takes place in two stages, which can be characterized in the following form:

$$\text{Stage} \quad \text{I} \quad \Rightarrow \quad \gamma^0 \rightarrow \gamma_{HC} + \alpha \tag{1}$$

$$\text{Stage} \quad \text{II} \quad \Rightarrow \quad \gamma_{HC} \rightarrow \alpha + \text{carbides} \tag{2}$$

where: $\gamma^0$ – primary austenite, $\gamma_{HC}$ – stable austenite (high carbon), $\alpha$ – plate ferrite.

Primary austenite $\gamma^0$ with the lowest carbon content is transformed into supersaturated ferrite plates and high-carbon austenite $\gamma_{HC}$. This process begins at the phase boundaries: graphite-austenite, austenite-austenite and previously formed ferrite plates [5]. During the growth of ferrite plates, the carbon diffuses into the austenite remaining between them, until it stabilizes. The end of the austenite saturation with carbon to a certain concen-

* WARSAW UNIVERSITY OF LIFE SCIENCES, FACULTY OF PRODUCTION ENGINEERING, 166 NOWOURSYNOWSKA STR., 02-787 WARSZAWA, POLAND
** WARSAW UNIVERSITY OF TECHNOLOGY, FACULTY OF PRODUCTION ENGINEERING, 85 NARBUTTA, 02-524, WARSZAWA POLAND
*** WARSAW UNIVERSITY OF TECHNOLOGY, FACULTY OF MATERIALS SCIENCE, 141 WOŁOSKA STR., 02-507 WARSZAWA, POLAND
# Corresponding author: cyprian_suchocki@sggw.pl

tration and the transition to the stability period of the mixture: $\alpha + \gamma_{HC}$ (ausferrite) begins the so-called "processing window" – time interval $t_{i1} \div t_{i2}$ [5]. Overheating longer than $t_{i2}$ results in the release of carbides, which are an undesirable phase in the ADI microstructure. During transformation at a temperature of 350÷400°C, after reaching $t_{i2}$ carbide $\varepsilon$ or cementite is released at the interface $\alpha/\gamma_{HC}$, leading to the formation of the microstructure characteristic of upper bainite (Fig. 1a). Decreasing the temperature of isothermal transformation reduces the amount of austenite and widens the "processing window" (Fig. 1b) [6]. Exceeding $t_{i2}$ time for this temperature is associated with the formation of lower bainite with ferrite morphology in the form of plates with a thickness of several dozen to several hundred nanometres. The low transformation temperature reduces the diffusion rate and prevents the transport of carbon atoms over long distances, which results in the formation of carbides not only on the $\alpha/\gamma_{HC}$ boundaries, but also in ferrite.

The studies performed for various types of ductile iron indicate a significant influence of chemical composition (especially alloy additions), austenitizing temperature and austempering temperature on the range of the "processing window" [4,10]. Studies show that increasing the content of alloying elements increases the time and reduces the temperature of stable "processing window". The increase in the austenitizing temperature has a similar effect.

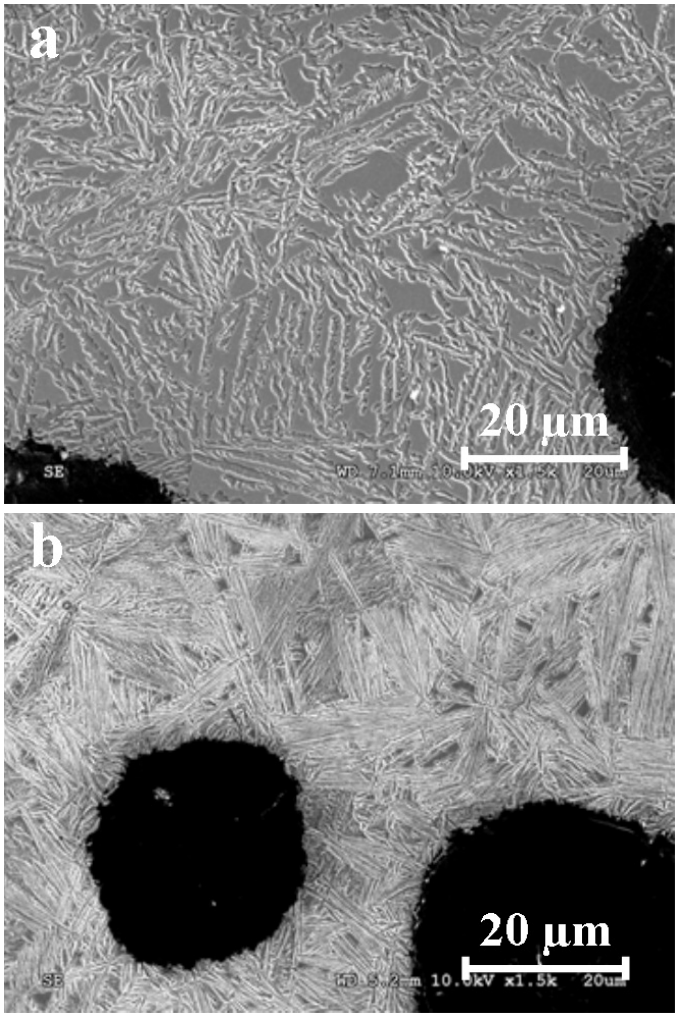


Fig. 1. Ductile iron microstructure in the „processing window" $t_{i1} \div t_{i2}$; a) temperature of isothermal transformation $T_i = 370$°C; b) temperature of isothermal transformation $T_i = 300$°C

### 2.2. Transformation kinetics modeling

A number of transformation kinetics equations has been applied to describe the isothermal ferrite growth which occurs in the ductile iron during austempering. Such changes in the structure of cast iron have not been the subject of modeling so far, which is why the article attempts to determine the possibilities and tools of mathematical description and prediction of changes which are described in this paragraph. The basic notions of the utilized models are gathered below.

#### 2.2.1. Johnson-Mehl-Avrami-Kolmogorov (JMAK) model

The JMAK kinetics equation which describes an isothermal phase growth has the following form [3,8,9,12,13]:

$$F(t) = \bar{F}(T)\left[1 - e^{-C(T)t^{n(T)}}\right] \tag{3}$$

where $F(t)$ is the transformed phase volume fraction at the time instant $t$, $\bar{F}(T)$ is the maximum volume fraction of the growing phase in the given temperature $T$, whereas $C(T)$ and $n(T)$ are the temperature-dependent parameters of JMAK model. An experimentally determined curve of the phase growth in temperature $T$ allows one to calculate the kinetics parameters using the following formulas:

$$n = \frac{\ln\left(\dfrac{\ln\left(1 - F_\alpha / \bar{F}\right)}{\ln\left(1 - F_\beta / \bar{F}\right)}\right)}{\ln\left(\dfrac{t_\alpha}{t_\beta}\right)}, \quad C = -\frac{\ln\left(1 - F_\alpha / \bar{F}\right)}{t_\alpha^n} \tag{4}$$

where: $t_\alpha$ – the nucleation time, $t_\beta$ – time of the transformation's finish, whereas $F_\alpha$ and $F_\beta$ are the initial and final volume fractions of ferrite. It is usually assumed that $\frac{F_\alpha}{\bar{F}} = 0.01$ and $\frac{F_\beta}{\bar{F}} = 0.99$. Alternatively, the values of $C$ and $n$ can be evaluated by the curve-fitting of experimentally measured phase growth data. For that purpose, the least squares method can be utilized.

#### 2.2.2. Austin-Rickett model

The transformation kinetics equation which was proposed by Austin and Rickett [2] is given as:

$$F(t) = \bar{F}(T)\left\{1 - \frac{1}{\left[k(T)t\right]^{n(T)} + 1}\right\} \tag{5}$$

with $k(T)$ and $n(T)$ being the model parameters which have to be determined based on the experimental measurements.

### 2.2.3. Starink model

The transformation kinetics equation proposed by Starink [15] has the following form:

$$F(t) = \bar{F}(T)\left[1 - \left\{\frac{\left[k(T)t\right]^{\eta(T)}}{\eta(T)} + 1\right\}^{-\eta(T)}\right] \tag{6}$$

where: $k(T)$, $n(T)$ and $\eta(T)$ are the temperature-dependent parameters of the model. It should be noted that in the case of $\eta = 1$ the Starink model is reduced to the Austin-Rickett equation.

### 2.3. Experiments

The material used in this study was obtained in the experimental foundry of the Institute of Manufacturing Processes WUT, using a medium frequency 40 kg capacity induction furnace. The chemical composition of ductile iron used in this investigation was as follows; C: 3.40%, Si: 2.80%, S: 0.015%, P: 0.035%, Mg: 0.055%, Mn: 0.28%, Cu: 0.72%, Mo: 0.27% Fe: bal. The material was originally cast in the form of Y-blocks with 25 mm thickness at the base of the ingot. After machining cylindrical ductile iron specimens with a diameter of 3 mm and a length of 10 mm, the specimens were subjected to the heat treatment processes, i.e. the austenitizing at 900°C/20 min. and the isothermal hardening at temperatures in the range: 270÷550°C. The processes were carried out using the Bahr DIL 805 Pro dilatometer. During the dilatometric experiments the specimen's increase in length corresponded to the change of the volume fraction of growing phase. In order to determine the final volume fraction of ferrite, the magnetic balance measurements were performed on the specimens. For that purpose, a sample magnetometer by Lake Shore Cryotronics Inc. was utilized.

## 3. Results

The Fig. 2 depicts the comparison of theoretical predictions generated by the JMAK model and the experimental measurements of ferrite growth in austempered ductile iron for selected temperatures. In the first approach (denoted as model 1 in Fig. 2), the parameter $C$ and $n$ values were determined by the approximation of experimental data. For that purpose, the least squares method and Scilab software was utilized. The residual sum of squares (RSS) is used as the measurement of curve fitting's quality. The values of RSS have been attached in Fig. 2. The determined kinetic constant values have been collected in Table 1. In the second approach (denoted as model 2 in Fig. 2). The values of $C$ and $n$ parameters were calculated for each temperature using equations (4).

The comparison of experimental data and simulated ferrite growth according to the Austin-Rickett model is shown in Fig. 3. The parameters of the model, $k$ and $n$ were evaluated by taking advantage of the least squares method. The obtained values of RSS are included in the figure. The determined kinetic constants have been gathered in Table 2.

TABLE 1

Parameters of JMAK equation determined for different temperatures

| Temperature (°C) | Parameter | |
|---|---|---|
| | $C$ ($s^{-1}$) | Avrami exponent $n$ |
| 550 | $0{,}53004\times10^{-2}$ | 1,0118 |
| 500 | $0{,}477\times10^{-2}$ | 0,948 |
| 450 | $0{,}246\times10^{-3}$ | 1,451 |
| 400 | $0{,}256\times10^{-3}$ | 1,327 |
| 370 | $0{,}2047\times10^{-3}$ | 1,329 |
| 350 | $0{,}446\times10^{-4}$ | 1,558 |
| 325 | $0{,}21\times10^{-4}$ | 1,634 |
| 270 | $0{,}2\times10^{-6}$ | 2,1083 |

TABLE 2

Parameters of Austin-Rickett equation determined for different temperatures

| Temperature (°C) | Parameter | |
|---|---|---|
| | $k$ ($s^{-1}$) | $n$ |
| 550 | $0{,}8406\times10^{-2}$ | 1,735 |
| 500 | $0{,}526\times10^{-2}$ | 1,642 |
| 450 | $0{,}411\times10^{-2}$ | 2,5042 |
| 400 | $0{,}262\times10^{-2}$ | 2,256 |
| 370 | $0{,}2307\times10^{-2}$ | 2,176 |
| 350 | $0{,}215\times10^{-2}$ | 2,142 |
| 325 | $0{,}179\times10^{-2}$ | 2,444 |
| 270 | $0{,}739\times10^{-3}$ | 3,325 |

In Fig. 4 the theoretical predictions of the Starink model are plotted against the experimentally measured ferrite fraction for the selected temperatures. The model parameters $k$, $n$ and $\eta$ have been determined using the least squares method. The values of RSS are attached in the figure. The evaluated values of the model parameters are collected in Table 3.

TABLE 3

Parameters of Starink equation determined for different temperatures

| Temperature (°C) | Parameter | | |
|---|---|---|---|
| | $k$ ($s^{-1}$) | $n$ | $\eta$ |
| 550 | $0{,}789\times10^{-2}$ | 1,549 | 1,292 |
| 500 | $0{,}614\times10^{-2}$ | 2,312 | 0,566 |
| 450 | $0{,}371\times10^{-2}$ | 2,02081 | 1,827 |
| 400 | $0{,}259\times10^{-2}$ | 2,197 | 1,0595 |
| 370 | $0{,}243\times10^{-2}$ | 2,461 | 0,785 |
| 350 | $0{,}274\times10^{-2}$ | 4,254 | 0,337 |
| 325 | $0{,}235\times10^{-2}$ | 5,744 | 0,264 |
| 270 | $0{,}699\times10^{-3}$ | 2,886 | 1,516 |

The maximum volume fractions of ferrite that have been measured for the considered temperatures of austempering using the magnetic balance method are given in Table 4.

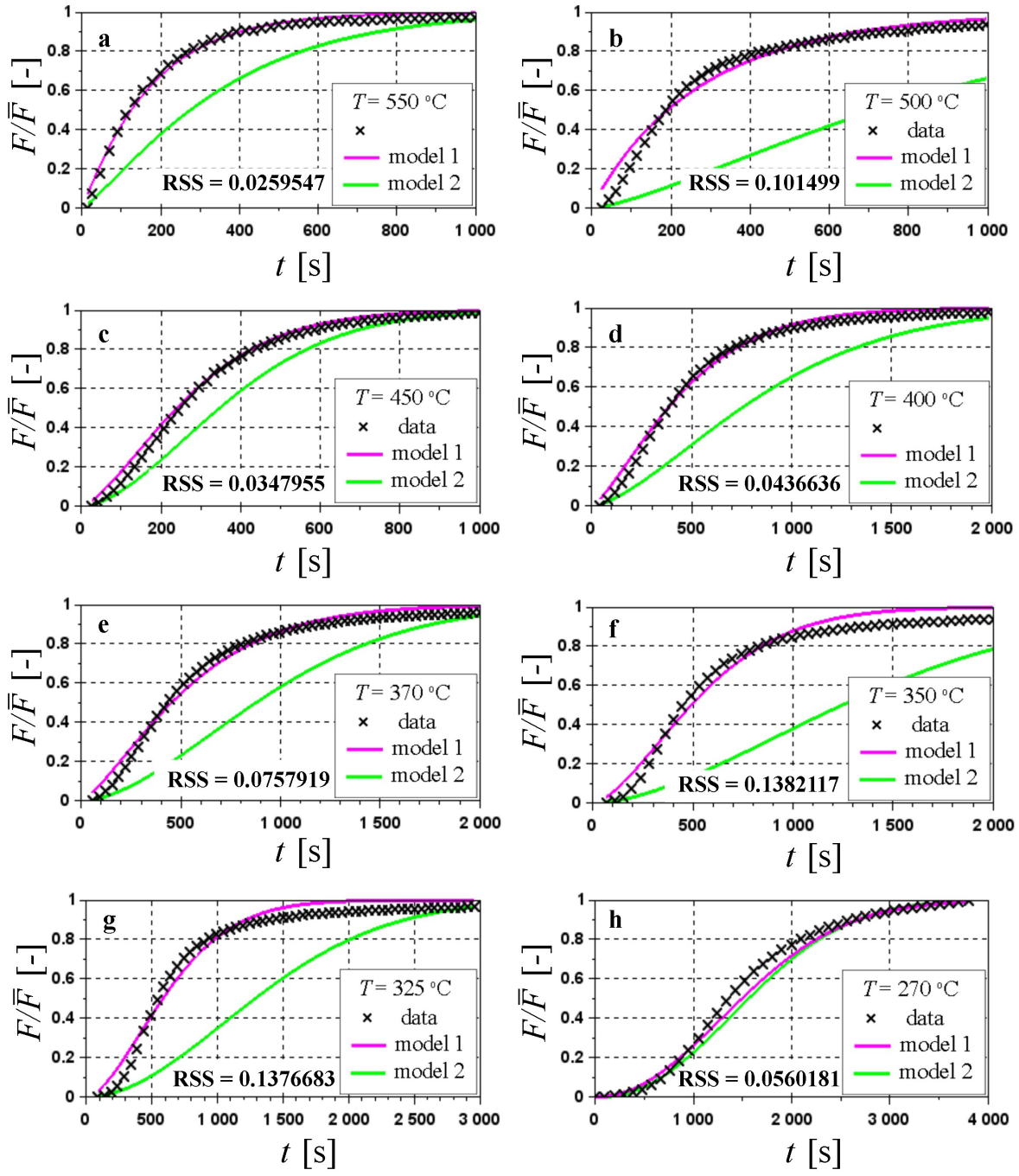


Fig. 2. Comparison of JMAK model predictions and experimental measurements of ferrite growth in austempered ductile iron and selected temperatures: model 1 – theoretical curves obtained for kinetic constants evaluated using least squares method, model 2 – theoretical curves obtained for kinetic constants calculated from equations (4)

TABLE 4

Maximum volume fraction of ferrite for selected temperatures

| Temperature (°C) | $\bar{F}$ |
|---|---|
| 550 | 0,996 |
| 500 | 0,992 |
| 450 | 0,800 |
| 400 | 0,616 |
| 370 | 0,651 |
| 350 | 0,721 |
| 325 | 0,7501 |
| 270 | 0,795 |

## 4. Conclusions

The best approximations of the experimentally measured ferrite growth during austempering of ductile iron were achieved for the Starink model (Fig. 4). Slightly worse results were obtained for the Austin-Rickett model (Fig. 3). The vastly used JMAK equation led to the least accurate curve fitting of the experimental data (Fig. 2) among the considered kinetic equations. It should be noted that calculating the kinetic constant $C$ and $n$ values according to the equations (4) usually leads to serious discrepancies between the measured and the simulated

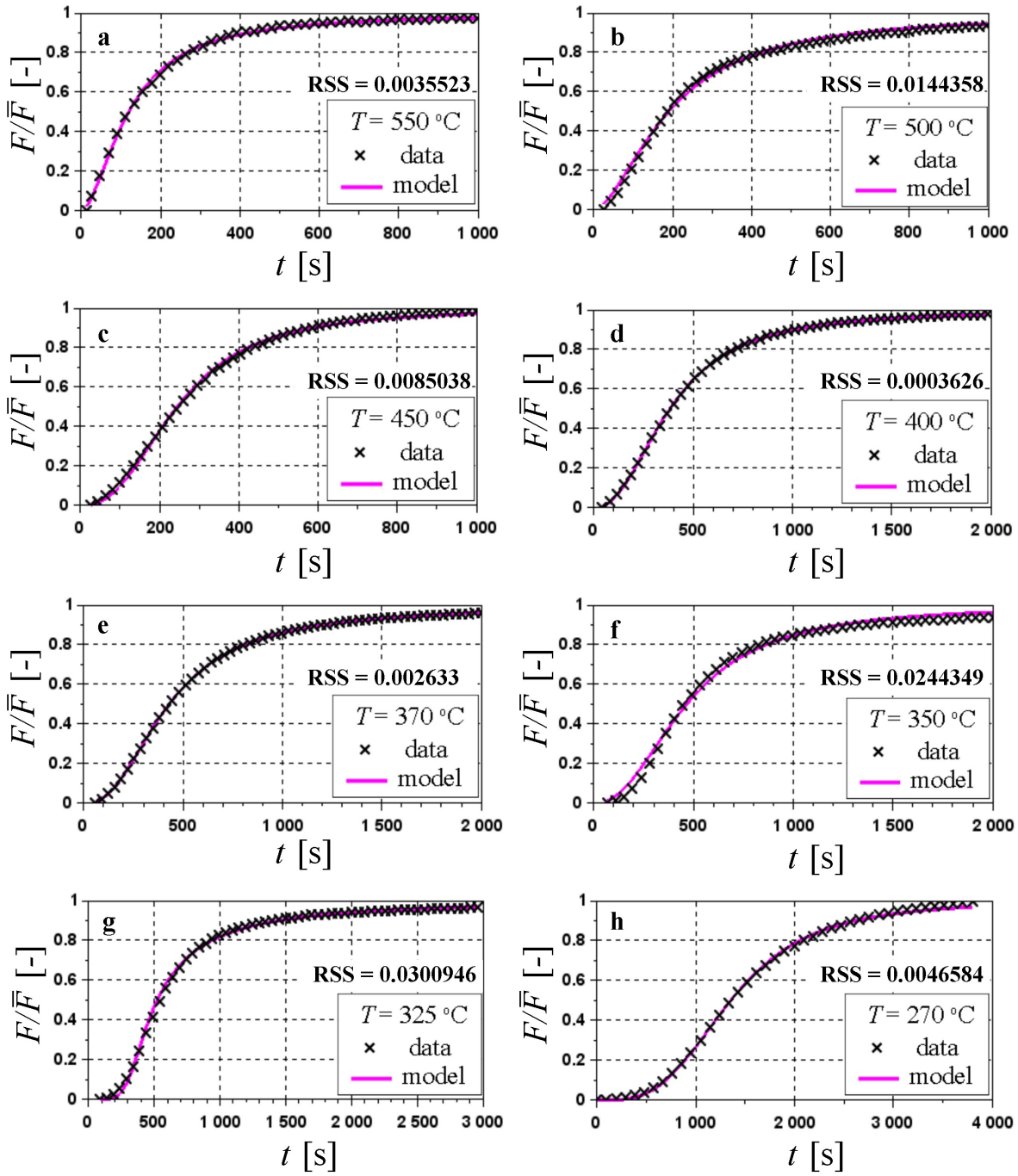


Fig. 3. Comparison of Austin-Rickett model predictions and experimental measurements of ferrite growth in austempered ductile iron and selected temperatures

ferrite fraction over time. Due to the measurement errors, the data points collected during a dilatometric experiment does not lie on a single analytical curve. This fact in most cases prevents calculating the correct values of JMAK equation's parameters by the utilization of equations (4). A significant improvement in the performance of JMAK model can be achieved when the kinetic constants are determined utilizing the least squares method.

The presented methodology can be generalized in order to describe the ferrite growth which occurs in ductile iron during the non-isothermal processes. Subsequently, such a generalization could be used in engineering software dedicated for simulating quenching and hot metal forming.

**Acknowledgements**

This work was supported by NCBiR project PBS III/B5/45/2015.

REFERENCES

[1] P.K. Agarwal, J.K. Brimacombe, Met. Trans. B **12B**, 121-133 (1981).

[2] J.B. Austin, R.L. Rickett, Trans. Am. Inst. Min. Metall. Eng. **135**, 396-443 (1939).

[3] M. Avrami, J. Chem. Phys. **7** (12), 1103-1112 (1939).

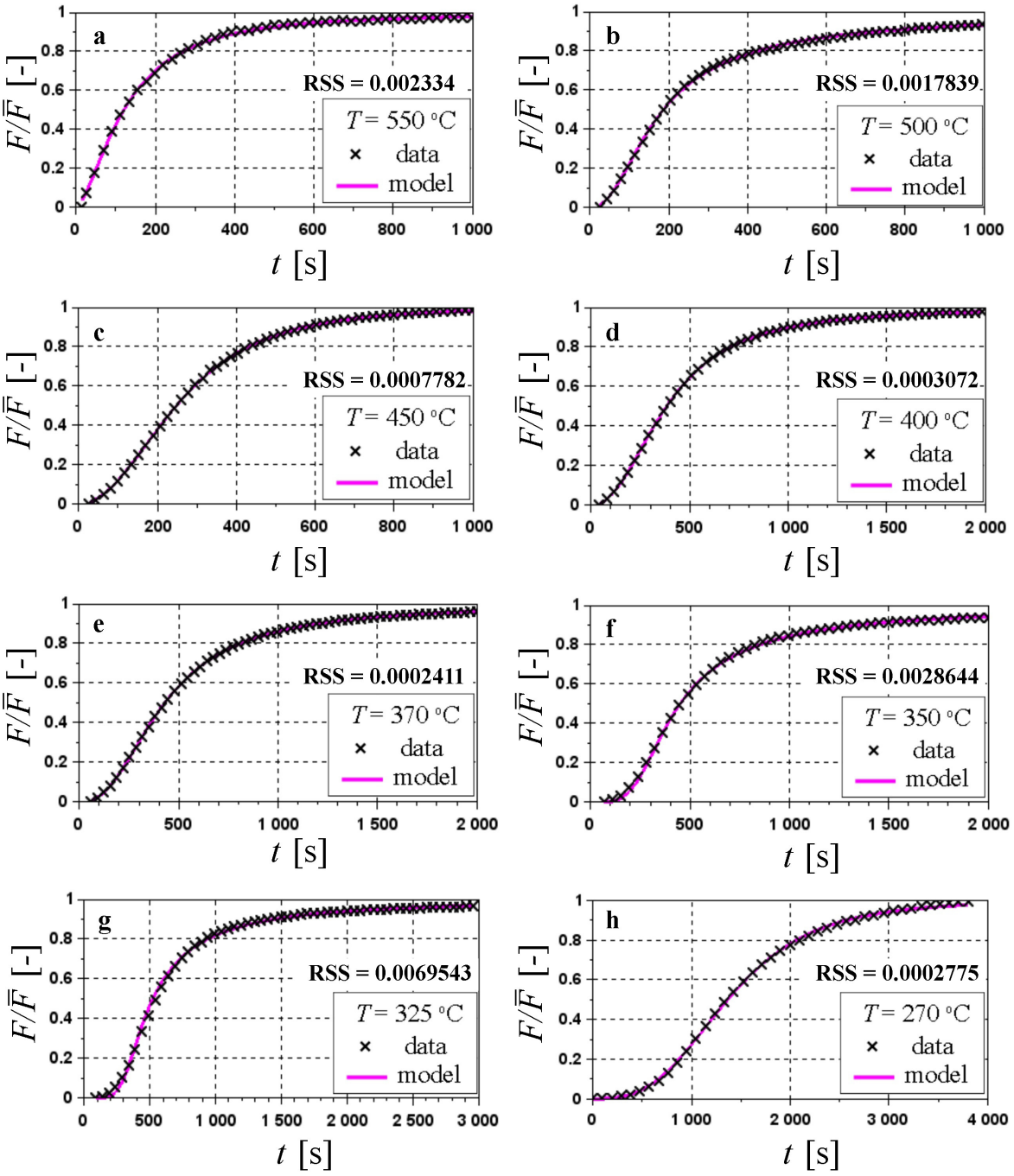


Fig. 4. Comparison of Starink model predictions and experimental measurements of ferrite growth in austempered ductile iron and selected temperatures


[4] H. Bayati, R. Elliot, Mater. Sci. Tech. **11** (8), 776-786 (1995).

[5] G. Cinceros, L. Perez, C. Campos, C. Valdes, Int. J. Cast Metal Res. **11** (5), 425-430 (1999).

[6] N. Darwish, R. Elliot, Mater. Sci. Tech. **9** (10), 572-586 (1993).

[7] A. Gazda, J. Therm. Anal. Cal. **102** (3), 923-930 (2010).

[8] A. Gazda, Therm. Acta **499**, 144-148 (2010).

[9] E. Guzik, M. Sokolnicki, A. Nowak, Arch. Fdy. Eng. **16** (2), 79-84 (2016).

[10] Liu Jincheng, R. Elliot, Int. J. Cast Metal Res. **12** (3), 189-195 (1999).

[11] S. Jemioło, M. Gajewski, Sci. Surv. Warsaw Univ. Tech., Civ. Eng. **143** (2005).

[12] W.A. Johnson, R.F. Mehl, Trans. Am. Inst. Min. Metall. Eng. **135**, 316-458 (1939).

[13] A.N. Kolmogorov, Izv. Akad. Nauk SSSR, Ser.Mat. **3**, 355-359 (1937).

[14] D. Myszka, M. Ahmed, A. Nofal, E. Skołek, A. Hussein, Mater. Sci. Fr. **925**, 210-217 (2018).

[15] M.J. Starink, J. Mater. Sci. **36**, 4433-4441 (2001).